Protein Science (1998), 7:1620–1625. Cambridge University Press. Printed in the USA.

FOR THE RECORD

Structure and stability of the P93G variant of ribonuclease A

L. WAYNE SCHULTZ, STEVEN R. HARGRAVES, TONY A. KLINK, AND RONALD T. RAINES

Departments of Biochemistry and Chemistry, University of Wisconsin–Madison, Madison, Wisconsin 53706

(RECEIVED October 27, 1997; ACCEPTED March 31, 1998)

Abstract: The peptide bonds preceding Pro 93 and Pro 114 of bovine pancreatic ribonuclease A (RNase A) are in the *cis* conformation. The *trans*-to-*cis* isomerization of these bonds had been indicted as the slow step during protein folding. Here, site-directed mutagenesis was used to replace Pro 93 or Pro 114 with a glycine residue, and the crystalline structure of the P93G variant was determined by X-ray diffraction analysis to a resolution of 1.7 Å. This structure is essentially identical to that of the wild-type protein, except for the 91–94 β-turn containing the substitution. In the wild-type protein, the β-turn is of type VIa. In the P93G variant, this turn is of type II with the peptide bond preceding Gly 93 being *trans*. The thermal stabilities of the P93G and P114G variants were assessed by differential scanning calorimetry and thermal denaturation experiments monitored by ultraviolet spectroscopy. The value of $\Delta\Delta G_m$, which reports on the stability lost in the variants, is 1.5-fold greater for the P114G variant than for the P93G variant. The greater stability of the P93G variant is likely due to the relatively facile accommodation of residues 91–94 in a type II turn, which has a preference for a glycine residue in its $i + 2$ position.

Keywords: β-turn; *cis* proline; endonuclease; protein stability; ribonuclease A; X-ray crystallography

The *cis* and *trans* isomers of Xaa–Pro peptide bonds differ in free energy by only 0.5 kcal/mol (Maigret et al., 1970). This isogenicity is the result of similar steric clashes between $C_{\alpha-1}$ and C_α in the *cis* (or *E*) conformation and between $C_{\alpha-1}$ and C_δ in the *trans* (or *Z*) conformation. Accordingly, 6% of Xaa–Pro peptide bonds in known protein structures are *cis* (MacArthur & Thornton, 1991). Moreover, the kinetic barrier to rotation of an Xaa–Pro peptide bond is low enough to allow for equilibration of the isomers in an unfolded protein, but high enough to limit the rate of protein folding. In contrast, the *cis* and *trans* isomers of nonprolyl peptide bonds differ in free energy by approximately 2.5 kcal/mol (Radzicka et al., 1988). The greater difference arises from the absence of a steric clash in the *trans* conformation. Although conformational constraints can force a nonprolyl peptide bond to be *cis* (Ramachandran & Venkatachalam, 1968), only 0.05% of nonprolyl peptide bonds are *cis* in known protein structures (Stewart et al., 1990). Most of these bonds are near the active sites of enzymes (Herzberg & Moult, 1991).

Bovine pancreatic ribonuclease A (RNase A; EC 3.1.27.5) has served as an important model system for elaborating protein structure–function relationships (D'Alessio & Riordan, 1997; Raines, 1998). Early pH-jump refolding experiments lead to the discovery that the folding pathway of RNase A contains a mixture of conformers with different folding rates (Garel & Baldwin, 1973). Soon thereafter, it was suggested that the slow-folding conformers are the result of *cis*-to-*trans* isomerization of the peptide bonds of Pro 93 and Pro 114 (Brandts et al., 1975), which are *cis* in native RNase A (Kartha et al., 1967).

Pro 93 and Pro 114 are located in type VI turns in solvent-exposed loops of RNase A (Fig. 1). The rate of unfolding of P93A RNase A is greater than that of the wild-type protein (Schultz & Baldwin, 1992; Dodge & Scheraga, 1996). It was suggested that this increase in unfolding rate is likely to be a result of the Ala 93 peptide bond being *cis* in the native state and isomerizing quickly to *trans* during unfolding. Likewise, the *trans*-to-*cis* isomerization of the Ala 93 peptide bond appears to limit the refolding rate of the fully denatured protein. The absence of these effects in the P114A variant of RNase A suggests that the Ala 114 peptide bond is *trans* in the native protein (Dodge & Scheraga, 1996).

Such different consequences of replacing a residue having a *cis* peptide bond have also been observed in other proteins. In P202A carbonic anhydrase II (Tweedy et al., 1993) and P39A ribonuclease T_1 (Mayr et al., 1994), the *cis* peptide bonds of the wild-type proline residues are retained in the alanine variants. Yet, replacing a *cis* proline residue in Staphylococcal nuclease results in a *trans* peptide bond in alternative β-turn structures: type I for the P117T variant, and type I′ for the P117G and P117A variants (Hynes et al., 1989).

Reprint requests to: Ronald T. Raines, Department of Biochemistry, University of Wisconsin–Madison, 420 Henry Mall, Madison, Wisconsin 53706-1569; e-mail: raines@biochem.wisc.edu.

Abbreviations: CD, circular dichroism; DSC, differential scanning calorimetry; DTT, dithiothreitol; EDTA, ethylenediaminetetraacetic acid; pdb, Protein Data Bank, which is maintained by the Brookhaven National Laboratory (http://pdb.pdb.bnl.gov/); RNase A, bovine pancreatic ribonuclease A; T_m, midpoint of the thermal unfolding curve; Tris, tris(hydroxymethyl)aminomethane; UV, ultraviolet.

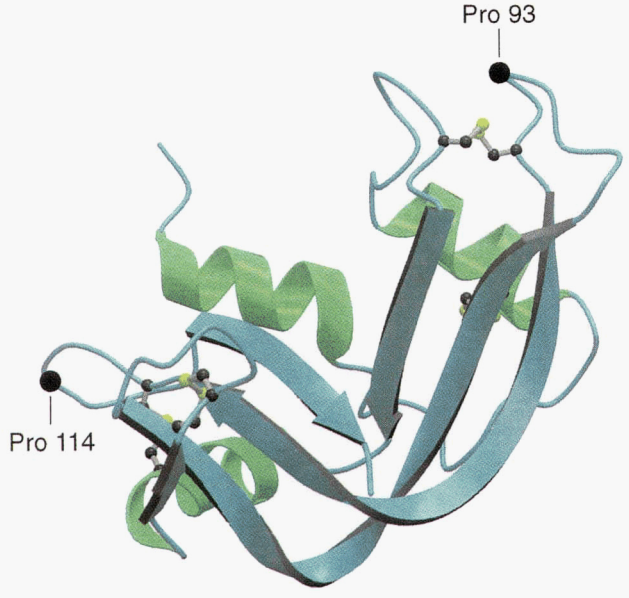

Fig. 1. Ribbon diagram of wild-type RNase A. Pro 93 and Pro 114 are located in solvent exposed type VI turns on opposite sides of the protein. The active site of RNase A lies in a deep cleft in the center of the protein between the N-terminal α-helix and central β-sheet. Disulfide bonds are represented in ball-and-stick format. The diagram was created with the programs MOLSCRIPT (Kraulis, 1991) and RASTER3D (Merritt & Murphy, 1994).

Previous studies have shown that the isomerization state of the peptide bond preceding residue 93 is an important determinant of the structure and stability of RNase A (Brandts et al., 1975; Schultz & Baldwin, 1992; Dodge & Scheraga, 1996). Yet, no structural data had been presented for variants at this position. We have used site-directed mutagenesis, X-ray diffraction analysis, and thermochemistry to provide new information about this residue. We report here the crystalline structure at 1.7 Å resolution of the P93G variant of RNase A. We also report the thermal stabilities of the P93G variant and, for comparison, the P114G variant.

Results and discussion: *Structure of P93G ribonuclease A:* RNase A has had a seminal role in the history of structural biology (for recent reviews, see Gilliland, 1997; González et al., 1997). RNase A was the fourth protein and third enzyme whose three-dimensional structure was determined by X-ray diffraction analysis (Kartha et al., 1967). The use of NMR spectroscopy in elaborating both protein structure (Saunders et al., 1957) and protein folding pathways (Udgaonkar & Baldwin, 1988) were developed with RNase A. The ^{1}H-NMR resonances of the protein have been assigned, and the structure of the enzyme in solution has been determined (Rico et al., 1989, 1991, 1993; Robertson et al., 1989). Altogether, over 70 sets of three-dimensional coordinates related to RNase A have been deposited in the Protein Data Bank (pdb) of the Brookhaven National Laboratory. Despite this historic success, no structures have been reported of RNase A variants created by site-directed mutagenesis. We have determined the first such structure.

We prepared a cDNA that codes for P93G RNase A by oligonucleotide-mediated site-directed mutagenesis of the wild-type cDNA. P93G RNase A was produced by expression of the mutant cDNA in *Escherichia coli*. Trigonal crystals of the purified P93G protein were grown at pH 6.0 in a concentrated salt solution. A single crystal was subjected to X-ray diffraction analysis. The resulting data set was 97% complete from 30 to 1.7 Å resolution, with an overall merging R-factor of 2.9%. The current R-factor from all data to 1.7 Å is 17.0%. The RMS deviations (RMSDs) from target geometries are 0.011 Å for bond lengths and 2.5° for bond angles.

The overall topology of P93G RNase A is the same as that of wild-type RNase A (pdb entry 1rph; Zegers et al., 1994). A least-squares superposition of the two structures results in a 0.38 Å RMSD of the main chains. The most significant deviation of the structures is in the 91–94 turn, which contains the amino acid substitution. The RMSD of the main chains is reduced to 0.35 Å when residues 91–94 are not included. The loop containing the 91–94 turn is located at one end of the protein, remote from the active site (Fig. 1), and is anchored to the rest of the protein by the Cys 26–Cys 84 and Cys 40–Cys 95 disulfide bonds.

We compare the structure of P93G RNase A to that of crystalline D121A RNase A (pdb entry 4rsd; Schultz et al., 1998). The D121A variant has a structure that is almost identical (0.37 Å RMSD of the main chain) to that of the crystalline wild-type protein in a concentrated salt solution (pdb entry 1rph). D121A RNase A was crystallized under conditions similar to those used to crystallize the P93G variant. The structure of D121A RNase A was refined to a higher resolution than was that of the wild-type protein and, because the D121A structure was solved in our laboratory, electron density maps were available for comparison. In wild-type RNase A and the D121A variant, the 91–94 turn is of type VIa with a *cis* peptide bond between Tyr 92 (i + 1) and Pro 93 (i + 2). There is a hydrogen bond of 2.9 Å (D121A) between the main-chain oxygen of Lys 91 (i) and the main-chain nitrogen of Asn 94 (i + 3) (Fig. 2), which is a common feature in a tight turn. The electron density of the D121A protein is continuous for the main chain and shows clearly that the Tyr 92–Pro 93 peptide bond is *cis*. The Tyr 92 and Pro 93 side chains are well defined, but the Lys 91 and Asn 94 side chains are disordered and do not appear in the map. This delineation has been reported for wild-type RNase A, as Zegers et al. (1994) observed weak electron density for residues 91–94 but no mutiple conformations. The ϕ,ψ torsional angles for Tyr 92 (−59°,144°) and Pro 93 (−80°,1°), along with ω = 1° for the peptide bond, are typical for a type VIa turn (Richardson, 1981) (Table 1). Additionally, the phenolic hydroxyl group of Tyr 92 forms a 2.6-Å hydrogen bond with the main-chain carbonyl of Lys 37, which is in an adjacent loop of the wild-type protein (Fig. 2). Otherwise, there are few interactions of the 91–94 turn with the rest of the protein, and there are no crystal contacts in the area that could influence the conformation of the turn.

In P93G RNase A, the 91–94 turn is of type II with a *trans* peptide bond between Tyr 92 and Gly 93 (Figs. 2 and 3). The ϕ,ψ torsional angles for Tyr 92 (−53°,126°) and Gly 93 (96°,-21°), along with ω = −179° for the peptide bond, are typical for a type II turn (Richardson, 1981) (Table 1). The $i \rightarrow i + 3$ hydrogen bond, now 2.5 Å, is conserved between the main-chain oxygen of Lys 91 and the main-chain nitrogen of Asn 94. The main chain is clearly defined and has continuous electron density, but the side chain of Lys 91 is disordered, and the side chain of Asn 94 is defined only weakly. A large negative peak in the $F_o - F_c$ difference map indicates that the side chain of Tyr 92 has changed its position significantly. A positive $F_o - F_c$ map was used to determine the direction in which the side chain is pointing, but density was

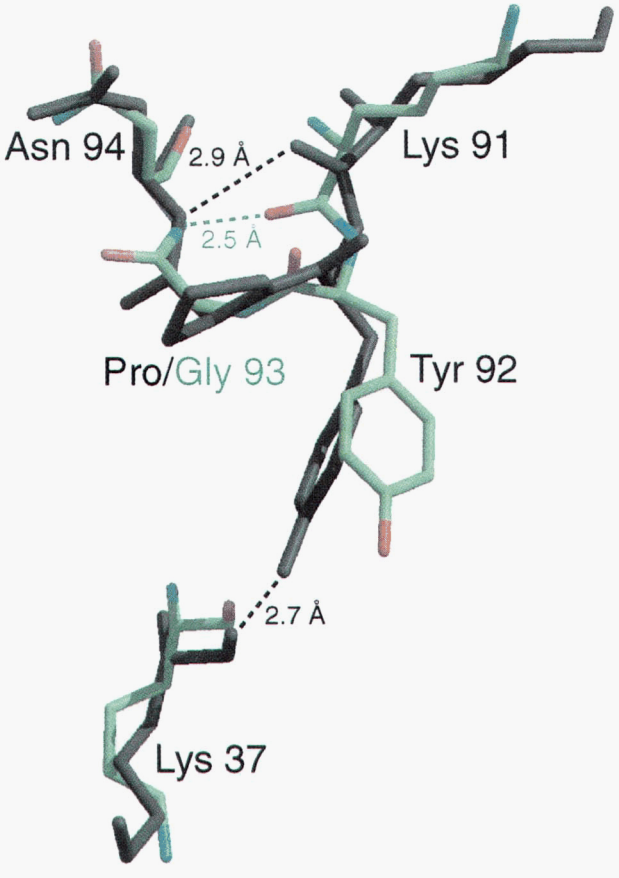

Fig. 2. Least-squares superposition of residues 37 and 90–94 of P93G RNase A (green) and D121A RNase A (black; pdb entry 4rsd; Schultz et al., 1998). Hydrogen bonds occurring in P93G RNase A (green) and D121A RNase A (black) are shown as dashed lines with the indicated lengths. This image was created with the program RASTER3D (Merritt & Murphy, 1994).

absent for most atoms. A conformational change in the turn has moved Tyr 92 into a position where it cannot form a hydrogen bond to the main-chain oxygen of Asn 37 (Fig. 2), and this change is likely to be responsible for the side-chain disorder.

Although glycine has much accessible conformational space, formation of a *cis* glycyl peptide bond is still destabilizing (Ramachandran & Venkatachalam, 1968). Nonetheless, the inherent conformational flexibility of glycine apparently allows the formation of a type II turn with all *trans* peptide bonds within the restricted 91–94 turn of RNase A. In contrast, kinetic studies on the unfolding/folding of the P93A variant suggest that Ala 93 retains a *cis* peptide bond (Schultz & Baldwin, 1992; Dodge & Scheraga, 1996). Apparently, a glycine residue but not a less flexible alanine residue can adopt a *trans* conformation in position 93. Moreover, we know of no protein structure in which an alanine residue occupies position $i + 2$ of a type II turn.

Stability of P93G RNase A and P114G RNase A: Replacing a residue with glycine usually decreases the thermal stability of a protein (Matthews, 1987). This decrease is likely to result from an increase in the entropy of the unfolded protein. In a folded protein, the number of conformational states available to proline and glycine residues is similar. But in an unfolded protein, a glycine residue has many more available conformational states than does a proline residue.

We determined the T_m (which is the midpoint of the thermal transition) of wild-type RNase A and the P93G and P114G variants by both differential scanning calorimetry (DSC) and thermal denaturation experiments monitored by ultraviolet (UV) spectroscopy. Data from the DSC and UV spectroscopy experiments were in strong agreement. These data show that P93G RNase A and P114G RNase A are significantly less stable than is wild-type RNase A. Our value of ΔT_m for P114G RNase A is similar to that reported by Schultz and Baldwin (1992) (Table 2), which was determined by circular dichroism (CD) spectroscopy. Dodge and Scheraga (1996) found that in comparison to replacing a proline residue with a *cis* peptide bond, replacing Pro 42 and Pro 117 (which are preceded by a *trans* peptide bond) is less destabilizing. The somewhat larger ΔT_m for the P117A variant may be due to its proximity to Pro 114 (Dodge & Scheraga, 1996).

The values of ΔT_m for P114G RNase A and P114A RNase A are similar, but the values for the P93G and P93A variants are different (Table 2) (Schultz & Baldwin, 1992; Dodge & Scheraga, 1996). What is the structural basis for this dichotomy? Pro 114 resides in a solvent exposed type VIb turn. This β-turn is on the opposite side

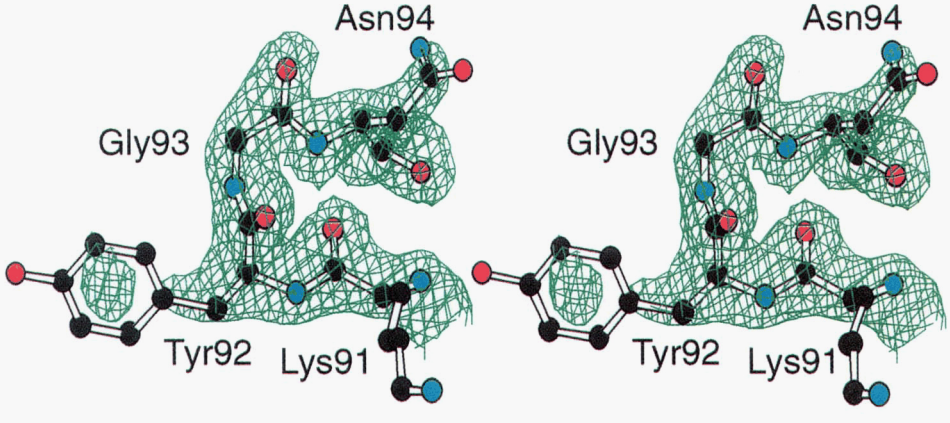

Fig. 3. Stereo view of the omit difference density ($2F_o - F_c$) for residues 91–94 of P93G RNase A contoured at 1.2σ over background. The density indicates that the peptide bond between Tyr 92 and Gly 93 is in the *trans* conformation.

Table 1. *Geometric parameters of residues in β-turns*

	Residues 92–93				Residues 113–114			
	$i+1$		$i+2$		$i+1$		$i+2$	
Structure	ϕ (°)	ψ (°)	ϕ (°)	ψ (°)	ϕ (°)	ψ (°)	ϕ (°)	ψ (°)
RNase A[a]	−64	130	−92	−2	−124	78	−85	134
D121A[b]	−59	144	−80	1	−144	110	−66	159
P93G[c]	−53	125	96	−21	−140	104	−64	153
Type I[d]	−60	−30	−90	0				
Type II[d]	−60	120	80	0				
Type VIa[d]	−60	120	−90	0				
Type VIb[d]					−120	120	−60	0

[a]Zegers et al. (1994).
[b]Schultz et al. (1998).
[c]This work.
[d]Richardson (1981).

of the protein from the 91–94 turn and is tethered to the rest of the protein by the Cys 58–Cys 110 disulfide bond. The ϕ,ψ torsional angles of Asn 113 (−144°,110°) and Pro 114 (−66°,159°) are typical for a type VIb turn. This turn does not form an $i \rightarrow i+3$ hydrogen bond, and has few contacts with the protein and none with symmetry partners in the crystal. Yet, the average *B*-factors for the main chain in this turn are relatively low (29.0 Å^2 for P93G; 29.1 Å^2 for D121A), which is consistent with a stable but perhaps fragile conformation. Dodge and Scheraga (1996) inferred from kinetic data that Ala 114 in the P114A variant has a *trans* peptide bond. Because the P114G and P114A variants are of equal stability, it is likely that the peptide bond of Gly 114 also adopts the *trans* conformation.

Table 2. *Thermodynamic parameters for the denaturation of wild-type RNase A and its variants*

Ribonuclease A	T_m (°C)	$-\Delta T_m$ (°C)	$-\Delta\Delta G_m$ (kcal/mol)
Wild-type[a]	61.6 (61.8)	—	—
P93G[a]	55.4 (54.5)	6.2 (7.3)	2.2 (2.6)
P114G[a]	52.1 (51.6)	9.5 (10.2)	3.3 (3.6)
Wild-type[b]	56.0	—	—
P93A[b]	46.5	9.5	2.7
P93S[b]	47.5	8.5	2.1
P114A[b]	45.5	10.5	3.2
P114G[b]	45.5	10.5	2.8
Wild-type[c]	44.4	—	—
P42A[c]	43.0	1.4	nd[d]
P93A[c]	33.7	10.7	nd
P114A[c]	33.8	10.6	nd
P117A[c]	37.7	6.7	nd

[a]This work. Values were determined by thermal denaturation experiments monitored by UV spectroscopy (±2 °C) or by DSC (±1 °C; in parentheses). UV spectroscopy experiments were performed in 30 mM sodium acetate buffer, pH 6.0, containing NaCl (0.10 M). DSC experiments were performed in H_2O.
[b]Schultz and Baldwin (1992). Values were determined by thermal denaturation experiments monitored by CD spectroscopy. Experiments were performed in 0.01 M sodium acetate buffer, pH 4.2, containing NaCl (0.1 M).
[c]Dodge and Scheraga (1996). Values were determined by thermal denaturation experiments monitored by UV spectroscopy. Experiments were performed in 50 mM sodium acetate buffer, pH 5, containing guanidinium chloride (1.3 M).
[d]Not determined.

P93G RNase A and P93A RNase A differ in their stabilities. It is likely that these two proteins, like the P114G and P114A variants, would have similar stabilities if the peptide bonds preceding Gly 93 and Ala 93 were in the same conformation. Thus, the favorable isomerization of residue 93 from *cis* in P93A RNase A to *trans* in P93G RNase A likely contributes to the greater stability of the P93G variant. Apparently, a glycine residue but not an alanine residue can occupy the $i+2$ position of a type II turn consisting of residues 91–94 of RNase A. The free energy lost upon replacing a *cis* proline residue in a β-turn with a *cis* alanine residue has been estimated to be 3.0 kcal/mol (Schultz & Baldwin, 1992; Tweedy et al., 1993). Apparently, this free energy is insufficient to isomerize the peptide bond preceding Ala 93 from *cis* to *trans* in the context of the 91–94 turn of RNase A.

Materials and methods: *Mutagenesis:* Plasmid pBXR directs the production of RNase A in *E. coli* (delCardayré et al., 1995). The cDNA that codes for RNase A was altered by oligonucleotide-mediated site-directed mutagenesis (Kunkel et al., 1987). The CCC codon for Pro 93 was replaced with the GGC codon (reverse complement underlined) for glycine using oligonucleotide RR53: 5′ CACAGTTGCCGTACTTGGAGCTCCCGGTCTC 3′, which also incorporates a translationally silent *Sac*I site (double underlined). The CCG codon for Pro 114 was replaced with the GGG codon for glycine using oligonucleotide RR18: 5′ AATGGACTG GTACGTACCCGTTTCCCTCA 3′, which also incorporates a translationally silent *Sna*BI site. The success of the mutagenesis was confirmed by DNA sequencing.

Protein production and purification: P93G RNase A and P114G RNase A were produced and purified by the methods of delCardayré et al. (1995) and Kim and Raines (1993) with the following

modifications. A culture of *E. coli* strain BL21/DE3, transformed with the appropriate vector, was grown to an optical density of 2.0. Expression was induced by addition of IPTG, and cells were collected 3–4 h after induction. After cell lysis by passage through a French pressure cell, inclusion bodies were collected by centrifugation and resuspended by stirring for 2 h in 20 mM Tris–HCl buffer, pH 8.0, containing guanidine-HCl (7 M), DTT (0.10 M), and EDTA (10 mM). The protein solution was diluted tenfold with 20 mM acetic acid and centrifuged to remove precipitant. The supernatant was dialyzed overnight against 20 mM acetic acid. The P93G and P114G variants were refolded by adding the protein solution (0.15 L) dropwise to 0.35 L of 0.10 M Tris-acetic acid buffer, pH 8.5, containing sodium chloride (0.10 M), reduced glutathione (1 mM), and oxidized glutathione (0.2 mM). After resting overnight at 20 °C, the sample was concentrated by ultrafiltration with a YM10 membrane (10,000 M_r cutoff; Amicon, Beverly, Massachusetts) and applied to a Superdex G-75 gel filtration column (Pharmacia, Uppsala, Sweden) in 50 mM sodium acetate buffer, pH 5.0, containing NaCl (0.10 M) and sodium azide (0.02% w/v). The major peak was pooled and applied directly to an HR10/10 Mono S cation exchange column (Pharmacia). The P93G and P114G variants were eluted from the column with a linear gradient (35 + 35 mL) of sodium chloride (0.15–0.35 M) in 20 mM sodium acetate buffer, pH 5.0.

Protein crystallization: Crystals of P93G RNase A were prepared by vapor diffusion using the hanging drop method. Drops (6 μL) of 50 mM sodium acetate buffer, pH 6.0, containing P93G RNase A (15 mg/mL), saturated ammonium sulfate (15% v/v), and saturated sodium chloride (25% v/v) were suspended over 0.5 mL wells containing 100 mM sodium acetate buffer, pH 6.0, containing saturated ammonium sulfate (30% v/v) and saturated sodium chloride (50% v/v). Crystals were grown at 20 °C, appeared within three days, and grew to a final size of 0.4 × 0.4 × 0.5 mm. For comparison, wild-type crystals were grown by equilibrating RNase A (35 mg/mL) in sodium phosphate (20 mM) and sodium acetate (20 mM) buffers, pH 6.0 with saturated ammonium sulfate (35% v/v) and sodium chloride (1.5 M) (Zegers et al., 1994).

Structural data collection: The crystals were of space group $P3_221$, with $a = 65.79$ Å, $c = 66.12$ Å, $\alpha = \beta = 90°$, and $\gamma = 120°$. X-ray data were collected with a Siemens HI-STAR detector mounted on a Rigaku rotating anode operating at 50 kV, 90 mA, and a 300-μm focal spot. The X-ray beam was collimated by double focusing mirrors. The crystal to detector distance was 12.0 cm. Data were obtained in 512 × 512 pixel format, processed using the program XDS (Kabsch, 1988a, 1988b), and scaled using the program XSCALIBRE (G.E. Wesenberg and I. Rayment, unpubl. obs.). Nine hundred 0.15° frames (135°) of data were collected from a single crystal using a single ϕ-scan. Only reflections with $I/\sigma >$ 0.33 were accepted, which resulted in the rejection of 31 from 19,167 unique reflections. The data have an average I/σ of 19.1 and an average redundancy of 2.6. The crystal was cooled in a 0.5° cold air stream resulting in negligible crystal decay for the entire data collection. The overall R_{sym} for all data in the resolution range 30–1.7 Å is 2.9% and for the highest resolution bin of 1.8–1.7 Å is 15.0%.

Structural data refinement: The starting model consisted of residues 1–124 of D121A RNase A (Schultz et al., 1998) that was stripped of all solvent molecules and residues 90–95. The model was subjected to 10 cycles of least-squares refinement using the program TNT (Tronrud et al., 1987), to give an initial R-factor of 24.0%. Manual adjustments to the model were performed using the program FRODO (Jones, 1985). After several cycles of manual adjustments and least-squares refinement, water molecules were added to the model. The peak searching algorithm in TNT was used to place ordered water molecules. Water molecules were retained if they had at least 1σ of $2F_o - F_c$ density and 3σ of $F_o - F_c$ density, and were within hydrogen bonding distance of the protein or other water molecules. Based on structures reported by Fedorov et al. (1996), two solvent molecules were determined to be chloride ions and have similar positions to those reported. The R-factor at this point was 18.5%. A difference Fourier map ($F_o - F_c$) clearly showed the position of the main chain for residues 90–95. The main-chain atoms for residues 90–95 were fitted to the density and revealed that the bond between residues 92 and 93 was *trans*. The side chains of residues 91, 92, and 94 were not clearly defined in the electron density map, so only those atoms with clear electron density were included in refinement. Side-chain atoms with no electron density were assigned an occupancy of 0.0 and modeled in a standard conformation. The final model contains the complete protein (residues 1–124), 129 water molecules, and 2 chloride ions. The average B-factors for the main- and side-chain atoms of P93G are 23 and 36 Å^2, respectively. The highest B-factors are found in the side chains of solvent exposed residues and exterior loops of the protein containing residues 37–38 and 87–95. The lowest B-factors are found in the hydrophobic core in residues 72–82. Atomic coordinates for P93G RNase A have been deposited in the pdb with accession code 3rsp.

Ultraviolet spectroscopy: UV spectroscopy was performed on a Cary 3 UV/visible spectrometer equipped with a Cary temperature controller. As RNase A is denatured, its six tyrosines become exposed to solvent resulting in a decrease of the molar absorptivity at 287 nm (Hermans & Scheraga, 1961). Thermal stability was assessed by monitoring the change in absorbance at 287 nm with temperature (Pace et al., 1989; Eberhardt et al., 1996). Solutions of protein (1 mg/mL) were prepared in 30 mM sodium acetate buffer, pH 6.0 containing NaCl (0.10 M). The absorbance at 287 nm was recorded as the temperature was increased from 25 to 90 °C in 1 °C increments, with a 5-min equilibration at each temperature. Similarly, the absorbance at 287 was recorded as the temperature was decreased from 90 to 25 °C. The data were fitted to a two-state model for denaturation, and T_m (the midpoint in the thermal denaturation curve) was calculated using the program SIGMA PLOT 4.16.

Differential scanning calorimetry: DSC was performed on a MicroCal Micro Calorimetry System (MCS) calorimeter at a scan rate of 1.0 °C min^{-1}. Protein solutions were dialyzed exhaustively against distilled deionized water. Protein solutions and a sample of the final dialysis solution were centrifuged at 15,300 × g to remove precipitants. The supernatants were degassed by vacuum. Protein concentrations (0.41–3.1 mg/mL) were determined immediately prior to sample cell loading. The centrifuged, degassed dialysis solution was used as the blank during blank versus blank and sample versus blank scanning. During scanning, samples were under nitrogen gas (30 psi). A single transition was observed in each DSC thermogram, and thermal denaturation was terminated approximately 20 °C past that transition. Denaturation was almost

completely reversible, as shown by rescanning samples a second time. Data collection and analysis were performed using the program ORIGIN (MicroCal Software, Northampton, Massachusetts).

The change in T_m caused by a small perturbation to a protein is related to the free energy of the perturbation ($\Delta\Delta G_m$) at the T_m of the unperturbed protein by the equation: $\Delta\Delta G_m = \Delta T_m \Delta S_m$, where the value of ΔS_m is for the unperturbed protein (Becktel & Schellman, 1987). This equation was used to calculate values of $\Delta\Delta G_m$ from data obtained by UV spectroscopy and DSC. The value of ΔS_m for wild-type RNase A was determined from the DSC data to be $\Delta S_m = \Delta H_m / T_m = 0.352$ kcal/(mol K), which is similar to that from UV spectroscopy data (Eberhardt et al., 1996).

Note added in proof: Subsequent to the submission of this manuscript, the crystalline structure of P93A RNase A was reported at a resolution of 2.3 Å [Pearson MA, Karplus PA, Dodge RW, Laity JHY, Scheraga HA. 1998. Crystal structures of two mutants that have implications for the folding of bovine pancreatic ribonuclease A. *Protein Sci 7*:1255–1258]. In that structure, the conformation of the Tyr92–Ala93 peptide bond is not unambiguous.

Acknowledgments: This work was supported by grant GM44783 (NIH). DSC data were obtained at the University of Wisconsin–Madison Biophysics Instrumentation Facility (http://www.biochem.wisc.edu/bif/BIF.html), which is supported by the University of Wisconsin–Madison and grant BIR-9512577 (NSF). L.W.S was supported by postdoctoral fellowship CA69750 (NIH). T.A.K. was supported by an Advanced Opportunity Fellowship from the University of Wisconsin–Madison. We thank Dr. D.R. McCaslin, O. Magnusson, S.R. Barrows, and M.L. Zupancic for assistance, B.M. Templer for advice, and Prof. W.J. Rutter for support of the early phases of this work. We are especially grateful to Prof. I. Rayment, Prof. H.M. Holden, and the members of their research groups for many helpful conversations and for the use of their X-ray data collection and computational facilities, which are supported by grant BIR-9317398 (NSF).

References

Becktel WJ, Schellman JA. 1987. Protein stability curves. *Biopolymers 26*:1859–1877.

Brandts JF, Halvorson HR, Brennan M. 1975. Consideration of the possibility that the slow step in protein denaturation reactions is due to *cis-trans* isomerism of proline residues. *Biochemistry 14*:4953–4963.

D'Alessio G, Riordan JF, eds. 1997. *Ribonucleases: Structures and functions*. New York: Academic Press.

delCardayré SB, Ribó M, Yokel EM, Quirk DJ, Rutter WJ, Raines RT. 1995. Engineering ribonuclease A: Production, purification, and characterization of wild-type enzyme and mutants at Gln11. *Protein Eng 8*:261–273.

Dodge RW, Scheraga HA. 1996. Folding and unfolding kinetics of the proline-to-alanine mutants of bovine pancreatic ribonuclease A. *Biochemistry 35*:1548–1559.

Eberhardt ES, Wittmayer PK, Templer BM, Raines RT. 1996. Contribution of a tyrosine side chain to ribonuclease A catalysis and stability. *Protein Sci 5*:1697–1703.

Fedorov AA, Joseph-McCarthy D, Fedorov E, Sirakova D, Graf I, Almo SC. 1996. Ionic interactions in crystalline bovine pancreatic ribonuclease A. *Biochemistry 35*:15962–15979.

Garel J-R, Baldwin RL. 1973. Both the fast and slow refolding reactions of ribonuclease A yield native enzyme. *Proc Natl Acad Sci USA 70*:3347–3351.

Gilliland GL. 1997. Crystallographic studies of ribonuclease complexes. In D'Alessio G, Riordan JF, ed. *Ribonucleases: Structures and functions*. New York: Academic Press. pp 305–341.

González C, Santoro J, Rico M. 1997. NMR solution structures of ribonuclease A and its complexes with mono- and dinucleotides. In: D'Alessio G, Riordan JF, ed. *Ribonucleases: Structures and functions*. New York: Academic Press. pp 343–381.

Hermans J Jr, Scheraga HA. 1961. Structural studies of ribonuclease. V. Reversible change of configuration. *J Am Chem Soc 83*:3283–3292.

Herzberg O, Moult J. 1991. Analysis of the steric strain in the polypeptide backbone of protein molecules. *Proteins Struct Funct Genet 11*:223–229.

Hynes TR, Kautz RA, Goodman MA, Gill JF, Fox RO. 1989. Transfer of a β-turn structure to a new protein context. *Nature 339*:73–76.

Jones TA. 1985. Diffraction methods for biological macromolecules. Interactive computer graphics: FRODO. *Methods Enzymol 115*:157–171.

Kabsch W. 1988a. Automatic indexing of rotation diffraction patterns. *J Appl Crystallogr 21*:67–71.

Kabsch W. 1988b. Evaluation of single-crystal X-ray diffraction data from a position-sensitive detector. *J Appl Crystallogr 21*:916–924.

Kartha G, Bello J, Harker D. 1967. Tertiary structure of ribonuclease. *Nature 213*:862–865.

Kim J-S, Raines RT. 1993. Bovine seminal ribonuclease produced from a synthetic gene. *J Biol Chem 268*:17392–17396.

Kraulis PJ. 1991. MOLSCRIPT: A program to produce both detailed and schematic plots of protein structures. *J Appl Crystallogr 24*:946–950.

Kunkel TA, Roberts JD, Zakour RA. 1987. Rapid and efficient site-specific mutagenesis without phenotypic selection. *Methods Enzymol 154*:367–382.

MacArthur MW, Thornton JM. 1991. Influence of proline residues on protein conformation. *J Mol Biol 218*:397–412.

Maigret B, Perahia D, Pullman B. 1970. Molecular orbital calculations on the conformation of polypeptides and proteins. IV. The conformation of the prolyl and hydroxyprolyl residues. *J Theor Biol 29*:275–291.

Matthews BW. 1987. Genetic and structural analysis of the protein stability problem. *Biochemistry 26*:6885–6888.

Mayr LM, Willbold D, Rösch P, Schmid FX. 1994. Generation of a non-prolyl *cis* peptide bond in ribonuclease T_1. *J Mol Biol 240*:288–293.

Merritt EA, Murphy MEP. 1994. Raster3D Version 2.0, a program for photorealistic molecular graphics. *Acta Crystallogr D50*:869–873.

Pace CN, Shirley BA, Thomson JA. 1989. Measuring the conformational stability of a protein. In Creighton TE, ed. *Protein structure*. New York: IRL Press. pp 311–330.

Radzicka A, Pedersen L, Wolfenden R. 1988. Influences of solvent water on protein folding: Free energies of solvation of *cis* and *trans* peptides are nearly identical. *Biochemistry 27*:4538–4541.

Raines RT. 1998. Ribonuclease A. *Chem Rev 98*:1045–1065.

Ramachandran GN, Venkatachalam CM. 1968. Stereochemical criteria for polypeptides and proteins. IV. Standard dimensions for the *cis*-peptide unit and conformation of *cis*-polypeptides. *Biopolymers 6*:1255–1262.

Richardson JS. 1981. The anatomy and taxonomy of protein structure. *Adv Protein Chem 34*:167–339.

Rico M, Bruiz M, Santoro J, González C, Neira JL, Nieto JL, Herranz J. 1989. Sequential ^{1}H-NMR assignment and solution structure of bovine pancreatic ribonuclease A. *Eur J Biochem 183*:623–638.

Rico M, Santoro J, González C, Bruix M, Neira JL, Nieto JL. 1993. Refined solution structure of bovine pancreatic ribonuclease A by ^{1}H NMR methods. *Appl Magn Reson 4*:385–415.

Rico M, Santoro J, González C, Bruix M, Neira JL, Nieto JL, Herranz J. 1991. 3D structure of bovine pancreatic ribonuclease A in aqueous solution: An approach to tertiary structure determination from a small basis of proton NMR NOE correlations. *J Biomol NMR 1*:283–298.

Robertson AD, Purisima EO, Eastman MA, Scheraga HA. 1989. Proton NMR assignments and regular backbone structure of bovine pancreatic ribonuclease A in aqueous solution. *Biochemistry 1989*:5930–5938.

Saunders M, Wishnia A, Kirkwood JG. 1957. The nuclear magnetic resonance spectrum of ribonuclease. *J Am Chem Soc 79*:3289–3290.

Schultz DA, Baldwin RL. 1992. *Cis* proline mutants of ribonuclease A. I. Thermal stability. *Protein Sci 1*:910–915.

Schultz LW, Quirk DJ, Raines RT. 1998. His···Asp catalytic dyad of ribonuclease A: Structure and function of the D121N, D121A, and wild-type enzymes. *Biochemistry 37*. In press.

Stewart DE, Sarkar A, Wampler JE. 1990. Occurrence and role of *cis* peptide bonds in protein structures. *J Mol Biol 214*:253–260.

Tronrud DE, Ten-Eyck LF, Matthews BW. 1987. An efficient general-purpose least-squares refinement program for macromolecular structures. *Acta Crystallogr A43*:489–501.

Tweedy NB, Nair SK, Paterno SA, Fierke CA, Christianson DW. 1993. Structure and energetics of a non-proline *cis*-peptidyl linkage in a proline-202 → alanine carbonic anhydrase II variant. *Biochemistry 32*:10944–10949.

Udgaonkar J, Baldwin R. 1988. NMR evidence for an early framework intermediate on the folding pathway of ribonuclease A. *Science 335*:694–699.

Zegers I, Maes D, Dao-Thi M-H, Poortmans F, Palmer R, Wyns L. 1994. The structures of RNase A complexed with 3′-CMP and d(CpA): Active site conformation and conserved water molecules. *Protein Sci 3*:2322–2339.